

A Tool Chain for Aero-Elastic Simulations*

Thomas Ludwig, Silvio Merazzi
SMR Engineering & Development, CH-2500 Bienne, Switzerland

Alain Gehri, Jan B. Vos
CFS Engineering, CH-1015 Lausanne, Switzerland

Beat Bucher, Michel Guillaume
RUAG Aerospace, CH-6032 Emmen, Switzerland

*Paper presented at the 12th Australian International Aerospace Congress
Melbourne, 19-22 March 2007

April 19, 2007

Abstract

A time-domain aero-elastic tool chain with energy-conservative multi-region geometric coupling algorithms is presented. The tool chain is capable of simulating static and dynamic aero-elastic problems with medium to high accuracy. Since it integrates separate fluid and structural solvers, the tool chain belongs to the staggered type where fluid and structural problems are solved separately, taking advantage of each code's advanced numerical features. The tool chain constitutes a useful complement to the frequency-domain simulation tools widely used in aero-elastic analysis and design. The use of the tool chain is illustrated by a coupled Navier-Stokes aerodynamic and structural analysis of a military aircraft wing under a high angle of attack configuration.

1 Introduction

Numerical simulations which embody aero-elastic coupling methods constitute a fundamental tool for the conception and validation of aircraft designs. They allow for detailed and relatively inexpensive investigations of a large number of effects related to fluid-structure interaction, such as the determination of aerodynamic loads, divergence and flutter. Flutter is increasingly a concern in modern aircraft design, as new, lightweight composite structures are being used and the flight envelope is being extended to flow regimes with significant transsonic characteristics. Especially for designs exhibiting moving shock boundaries, conventional aero-elastic tools based on linearised theory cannot predict flutter behaviour with sufficient accuracy. For these situations, a time-domain coupling method has to be used.

The coupled aerodynamic - structural problem can be solved with one single simulation program or it can be split into several sub-problems, solving the structural and the aero-

dynamic problem separately. While the solution with one single simulation program allows for – at least in theory – working with one single mesh, the approach is – in practice – not very popular.

The nature of the equations involved in the coupled simulation is inherently different and hence require different numerical treatment. One of the consequences of this is that the structural and the aerodynamic mesh are significantly different as to geometry, size, element or cells involved, and mesh density. Therefore, the coupled problem is split in separate sub-problems, each of which is formulated and solved by specialists in the respective fields and, consequently, solved with specialised simulation programs.

Computing the aero-elastic equilibrium of a structure involves many different tools. The diagram of Fig. 1 shows the different data (mesh, loads, displacements) for the fluid dynamics (CFD) and structure (CSM) meshes, and how they are related to each other by the different tools:

- The fluid dynamics solver computes a steady solution. One of the resulting variables is the pressure in each cell. The force extraction tool computes the aerodynamic loads on the fluid dynamics surface, given the fluid dynamics mesh and the pressure field.
- The force-mapping tool is used to transfer the aerodynamic loads to the structure mesh, combining the aerodynamic loads with other loads.
- The displacement-mapping tool transfers the displacements from the structure mesh to the surface grid points of the fluid dynamics mesh. It is closely related to the force-mapping tool.
- The volume-mesh deformation tool calculates new coordinates for all fluid dynam-

ics mesh points such that the cells of the mesh are “well enough” shaped to be used by the fluid dynamics solver for a subsequent fluid dynamics computation step.

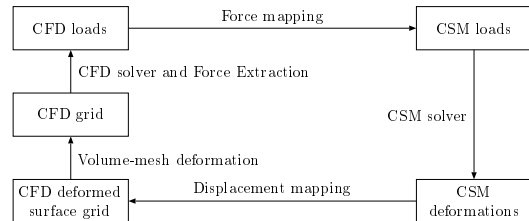


Figure 1: Tool chain used for computation of aero-elastic equilibrium.

When solving aero-elastic problems with different aerodynamic and structural meshes, one of the concerns of coupling meshes is the spatial coupling, which defines how the meshes and the associated variables, like deformations or pressures, are passed between the meshes. The spatial coupling will establish the rules for connecting points and elements of either mesh. One of the main concerns during the coupled simulation is the conservation of energy, is that particular emphasis has to be put on the selection of the interpolation methods. For realistic problems the complexity of spatial coupling is quite high. Especially for regions which exhibit differential deformations such as flaps and ailerons the mapping of the structure and the fluid meshes becomes very intricate. In addition, often only parts of the geometry are available, like points of clouds for the structural mesh. In addition, the mesh coupling process should produce a deformed fluid surface mesh which is continuous and, if possible, smooth such that the volume-mesh deformation can produce a valid and well-conditioned volume mesh for the subsequent aero-elastic iteration.

To enable multi-region geometric coupling while maintaining the aforementioned condi-

tions the FSCON and FSI tools have been created. The FSCON (Fluid-Structure CONnector) software is a graphical preprocessor for defining and linking the coupling regions on both the fluid surface and on the structural model. The FSI tool implements the multi-region geometric coupling algorithms discussed in this paper. Both tools are used in the context of static and dynamic aero-elastic simulations within the research and development programme of RUAG Aerospace for the F/A-18 fighter aircraft. The principal interest is to assess the loads in aero-elastic static and dynamic equilibrium for the Swiss F/A-18 fleet, with the ultimate goal of predicting aircraft lifetime.



Figure 2: F/A-18 fighter aircraft.

In this paper, emphasis is put on the static aero-elastic equilibrium problem; the ideas and concepts presented herein can be applied to dynamic simulations as well. For the simulation, the FSCON and FSI tools were used together with a Navier-Stokes multi-block CFD-solver [3], which also has volume-mesh deformation capability. The structural solver was MSC.-Nastran.

2 Geometric coupling

In most industrial applications of aero-elastic simulations, and in fluid-structure interaction in general, the fluid and structural problems are handled by different solvers, for the fluid problem by a CFD solver and for the structural problem by FEM based solvers. Consequently, the fluid and structural meshes do not match and they have to be brought in correspondence.

The term *geometric coupling* refers to techniques that relate fluid (surface) and structural degrees-of-freedom as a function of their locations. Thus, there is no need to establish a correspondence between the fluid and the structural degrees of freedom explicitly (by hand).

For the geometric coupling techniques discussed in this paper, fluid and surface models do not need to have matching boundaries, the structural response being, for many problems, predicted with sufficient accuracy by a reduced model. For example, in the FEM model of an aircraft, the wing is often reduced to the wing box section, with the leading edge and the trailing edge not being modelled at all. The geometric coupling part of fluid-structure interaction is then responsible for adding the missing parts.

In summary, due to geometric coupling, no additional modelling – the most time consuming task in structural and CFD analysis – is necessary. It is this convenience that renders geometric coupling tools so useful for the purpose of fluid-structure interaction.

2.1 Scattered-data interpolation

The geometric coupling techniques implemented in FSI and discussed in this paper belong to the class of scattered-data interpolation methods. Scattered-data interpolation has the advantage of versatility: It can be applied to any problem where the fluid surface and the structural model can be represented by sets of

nodes with concentrated forces and displacements defined at these nodes. In principle, no knowledge of any CAD surfaces, the FEM mesh connectivity, or the inner workings of the FEM model is required; whether the FEM model consists of shell or volume elements is largely irrelevant to the fluid-structure interaction, as long as the structural behaviour is described with sufficient accuracy by its translational degrees-of-freedom. Even a subset of the structural nodes can be chosen for the interaction with the fluid solver.

In the remainder of this paper we assume scattered data interpolation, translational displacements (no rotations), and concentrated nodal forces (no moments) as quantities to be exchanged between the structural domain and the fluid surface. Many of the concepts presented in the following can be extended to other interpolation techniques and to rotational or other types of degrees-of-freedom.

2.2 The geometric coupling operator

In scattered-data interpolation, the structure is represented by a set of data points with initial coordinates \mathbf{x}^s . At these data points, displacements \mathbf{u}^s from a previous structural FEM simulation shall be interpolated to the fluid surface.

The interpolation recipe is for any point x on the fluid surface:

$$u(x) = (\mathbf{g}(x, \mathbf{x}^s))^T \mathbf{u}^s$$

where u is the interpolated displacement at x and \mathbf{g} is a vector of influence coefficients, one for each data point. The influence coefficients are depend on x and on the initial coordinates of the data points.

All interpolants in FSI are exact at the support nodes:

$$\forall i \in \{1..N^s\} : u_i^s = (\mathbf{g}(x_i^s, \mathbf{x}^s))^T \mathbf{u}^s$$

Further, all interpolants are able to interpolate a constant field exactly:

$$c = (\mathbf{g}(x, \mathbf{x}^s))^T \begin{Bmatrix} c \\ c \\ \dots \end{Bmatrix}$$

Some of the algorithms are isoparametric as well:

$$x = (\mathbf{g}(x, \mathbf{x}^s))^T \mathbf{x}^s$$

The fluid surface is represented by set of fluid surface mesh nodes with initial coordinates \mathbf{x}^f . The linear operator G – the geometric coupling operator – is then obtained by evaluation of the interpolant g at each of the fluid surface nodes:

$$G = \begin{Bmatrix} \mathbf{g}(x_1^f, \mathbf{x}^s)^T \\ \mathbf{g}(x_2^f, \mathbf{x}^s)^T \\ \dots \end{Bmatrix}$$

Hence the fluid surface mesh displacements \mathbf{u}^f can be expressed as

$$\mathbf{u}^f = G\mathbf{u}^s \quad (1)$$

In practice, however, it is often more convenient and computationally more efficient to determine the fluid displacements (and vice-versa the structural forces) without explicitly computing the operator G .

2.3 Interpolation Methods

Scattered-data interpolation methods and their respective advantages and drawbacks are not discussed in this paper; we only mention a few classes of them:

- Interpolants making use of radial basis functions. There are many variants, and the literature is vast. For example, see [5] for an overview and [1] for their application to aero-elastic problems. For the interpolant used to obtain the results presented in this paper, refer to [6].

- Interpolants based on the Voronoi cell structure and its dual, the Dirichlet tessellation, formed by the data points and the interpolating point. Sibson’s interpolant [7] is an example.
- The constant-volume-tetrahedron method by Goura [2] has been designed for aircraft wings where only the wing box of the structure is modelled and the displacements must be extrapolated to the leading and trailing edges.

2.4 Conservation of work

When a structure deforms in function of fluid forces, the structural domain receives work from the fluid domain. The work, as calculated for the structural domain, must be equal to the work as calculated for the fluid (surface) domain. Conservation of work means that the geometric coupling scheme, and also in the case of unsteady fluid-structure interaction the temporal coupling scheme, do not absorb or emit any energy. We are concerned here with static equilibrium and the assumption of small (linear) displacements, hence the work for the fluid surface and the structure is

$$(\mathbf{u}^f)^T \mathbf{f}^f = (\mathbf{u}^s)^T \mathbf{f}^s \quad (2)$$

Not all geometric coupling algorithms satisfy (2). Depending on the type of analysis to be performed, conservation of work may become of great importance; this is particularly true for flutter simulations where otherwise the prediction of the flutter boundary will be biased. Since FSCON and FSI can be used for static and dynamic fluid-structure interaction, the geometric coupling techniques described in this paper and implemented in the FSI tool are designed such that the work is the same for the fluid and the structural domain even for multi-region coupling (see section 4).

For any geometric coupling scheme to preserve work, the following holds: Be G the coupling operator and $\mathbf{u}^f = G\mathbf{u}^s$, that is, G interpolates the fluid surface displacements \mathbf{u}^f from the structural displacements \mathbf{u}^s . Then, the transpose of that coupling operator G must be used for the transfer of the forces from the fluid surface to the structure: $\mathbf{f}^s = G^T \mathbf{f}^f$. Substitution into (2) yields

$$(G\mathbf{u}^s)^T \mathbf{f}^f = (\mathbf{u}^s)^T G^T \mathbf{f}^f$$

From this condition arises the following important consequence: The points on the fluid surface where one wishes to obtain the interpolated displacements \mathbf{u}^f , are also the points where the concentrated fluid surface forces must be specified. Since one cannot freely choose these points, they must be at the fluid surface mesh nodes as the displacements are sought for the latter. Thus, it is necessary to integrate the pressure field over the fluid surface to concentrated forces at the surface mesh nodes and, in a similar way, integrate the skin friction coefficients. Some CFD solvers already can generate such forces; for the NSMB CFD solver, which employs a cell-centred scheme, the corresponding integration functionality has been integrated in the NSMB-interface to FSI.

2.5 Total force

If G interpolates any constant field exactly and if G^T is used for the transfer of the loads, then total force is preserved in addition to work: For a uniform structural displacement field $\mathbf{u}^s = \{c, c \dots c\}^T$ with $c \neq 0$, the geometric coupling algorithm also yields a uniform fluid surface field $\mathbf{u}^f = \{c, c \dots c\}^T$. In this case we have for arbitrary \mathbf{f}^f

$$(\mathbf{u}^f)^T \mathbf{f}^f = \{c, c \dots c\} \mathbf{f}^f = c \sum \mathbf{f}^f = c \mathbf{f}_{\text{tot}}^f$$

and

$$(\mathbf{u}^s)^T \mathbf{f}^s = \{c, c \dots c\} \mathbf{f}^s = c \sum \mathbf{f}^s = c \mathbf{f}_{\text{tot}}^s$$

But since $(\mathbf{u}^f)^T \mathbf{f}^f = (\mathbf{u}^s)^T \mathbf{f}^s$, we have

$$\mathbf{f}_{\text{tot}}^f = \mathbf{f}_{\text{tot}}^s$$

2.6 Total moment

If G is isoparametric, that is, $\mathbf{x}^f = G\mathbf{x}^s$, and if G^T is used for the transfer of the loads, the total moment is preserved in addition to the total force and total work.

$$(\mathbf{x}^s)^T \times \mathbf{f}^s = (\mathbf{x}^s)^T \times (G^T \mathbf{f}^f) = ((\mathbf{x}^s)^T G^T) \times \mathbf{f}^f$$

But since $\mathbf{x}^f = G\mathbf{x}^s$, we have

$$(\mathbf{x}^f)^T \times \mathbf{f}^f = ((G\mathbf{x}^s)^T) \times \mathbf{f}^f = ((\mathbf{x}^s)^T G^T) \times \mathbf{f}^f$$

3 Boundary Conditions

For assumed displacement fields in structural FEM, natural boundary conditions describe forces, and essential boundary conditions describe imposed displacements. In geometric coupling, a force field \mathbf{f}^f and a displacement field \mathbf{u}^f are defined on the fluid surface. If one combines the geometric coupling and the structural solver into a “black box”, which, given a force field \mathbf{f}^f on the fluid surface, yields the corresponding equilibrium displacement field \mathbf{u}^f , then the forces \mathbf{f}^f are the natural boundary conditions, but a priori there are no essential boundary conditions defined on the fluid surface. The ability to specify essential boundary conditions on the fluid surface becomes important in the following cases:

- a For half models, nodes on the symmetry plane must remain on that symmetry plane. Ordinary interpolation methods will not fulfil that requirement by themselves.

- b If a part of a fluid model is not coupled with the structural model (for instance the structural model consists of a wing box, and the fluid model consists of a complete aircraft), then the displacements at the intersection to the uncoupled part of the fluid surface must be zero.

- c In multi-region coupling, for two adjacent regions, the displacements must be identical at the region intersection.

If any of these conditions is not satisfied, the subsequent volume-mesh deformation procedure will fail to produce a correct CFD volume mesh from the surface mesh displacements. Therefore, the FSCON tool permits the user to specify such essential boundary conditions for each coupling region. The FSI tool will generate the global coupling operator G such that these boundary conditions are respected while preserving work. This is explained in the following section.

3.1 Coupling procedure

We restrict our discussion to the case where the displacements are constrained to a fixed value or to a value of zero (conditions of type a and b). The procedure for essential boundary conditions of type c is described in section 4.

Let \mathbf{u}^c be the displacements at the constrained surface mesh nodes. Let \mathbf{u}^v be the displacements at the fluid surface mesh nodes that are not constrained (free)

$$\mathbf{u}^f = \left\{ \begin{array}{l} \mathbf{u}^c \\ \mathbf{u}^v \end{array} \right\}$$

Let \mathbf{u}^s be the displacements of the structural nodes. We want the totality of the fluid displacements, \mathbf{u}^f to be a continuous function. This is achieved by assigning the constrained nodes to the set of data points:

$$\mathbf{u}^v = \underbrace{[G^s \quad G^c]}_G \begin{Bmatrix} \mathbf{u}^s \\ \mathbf{u}^c \end{Bmatrix}$$

The forces are obtained by applying the transpose of G to the forces on the unconstrained fluid surface mesh nodes:

$$\begin{Bmatrix} \mathbf{f}^s \\ \bar{\mathbf{f}}^c \end{Bmatrix} = \underbrace{\begin{bmatrix} (G^s)^T \\ (G^c)^T \end{bmatrix}}_{G^T} \mathbf{f}^v$$

where $\bar{\mathbf{f}}^c$ are the forces acting on the constrained fluid surface mesh nodes *due to the constraints*. The total of the forces acting on the constrained nodes is $\bar{\mathbf{f}}^c + \mathbf{f}^c$. The forces at the structural nodes depend only on the forces at the unconstrained fluid mesh nodes, thus

$$\mathbf{f}^s = (G^s)^T \mathbf{f}^v$$

3.2 Total force and total moment

Since the coupling operator used to obtain the structural forces is not equal to the transpose of the operator used to obtain the fluid displacements, $G \neq (G_s)^T$, the total force and the total moment are in general not preserved:

$$\begin{aligned} \sum_i^{N^s} \mathbf{f}_i^s &= \sum_i^{N^v} \mathbf{f}_i^v - \sum_i^{N^c} \bar{\mathbf{f}}_i^c \\ \sum_i^{N^f} \mathbf{f}_i^f &= \sum_i^{N^v} \mathbf{f}_i^v + \sum_i^{N^c} \mathbf{f}_i^c \end{aligned}$$

3.3 Conservation of work

Work is in general not preserved, except if the constrained displacements are all zero, that is $\mathbf{u}^c = \{0, 0 \dots 0\}^T$. Then

$$(\mathbf{u}^f)^T \mathbf{f}^f = \{ (\mathbf{u}^v)^T \quad \mathbf{0} \} \begin{Bmatrix} \mathbf{f}^v \\ \mathbf{f}^c \end{Bmatrix} = (\mathbf{u}^v)^T \mathbf{f}^v$$

with

$$\mathbf{u}^v = \underbrace{[G^s \quad G^c]}_G \begin{Bmatrix} \mathbf{u}^s \\ \mathbf{0} \end{Bmatrix} = G^s \mathbf{u}^s$$

Hence

$$(\mathbf{u}^v)^T \mathbf{f}^v = (\mathbf{u}^s)^T (G^s)^T \mathbf{f}^v$$

Substitution of $\mathbf{f}^s = (G^s)^T \mathbf{f}^v$ finally yields equation (2):

$$(\mathbf{u}^f)^T \mathbf{f}^f = (\mathbf{u}^s)^T \mathbf{f}^s$$

Another exception occurs when the displacements for the constrained fluid surface mesh nodes are obtained from the structural displacements, that is $\mathbf{u}^c = G^c \mathbf{u}^s$. This is the case when inter-region continuity of the displacements is required, as described in section 4.

It is for this reason that FSCON and FSI only support zero-constraint and inter-region continuity constraints.

4 Multi-Region Coupling

The need for multi-region geometric coupling is apparent when control surfaces are present in the fluid and structural models. The movement of a control surface can be totally different from the movement of the neighbouring surfaces; for instance, a flap may rotate upwards due to the aerodynamic forces while the neighbouring wing section does not move much. Such discrepancies in deformation and deflection render any interpolation scheme useless if a single coupling region is used. In this case, the deflections are “disturbed”, since for obtaining the deformation on one part of the fluid surface, the interpolation takes into account also some of the neighbouring support points from the other parts. The less the density of the structural (support) points, the more pronounced this “parasite-coupling” effect becomes, see Fig. 3).

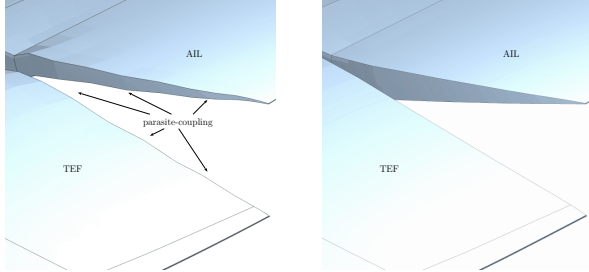


Figure 3: Parasite coupling (left) and multi-region coupling (right).

The remedy to this problem is multi-region coupling. A geometric coupling software with multi-region capabilities offers the possibility to define the different regions for both the fluid and the structural models. Since performing such a task by hand is tedious and error-prone, **FSCON**, the Fluid-Structure CONnector software, has been created. **FSCON** permits to display the fluid surface and the structural model together (for an example see Fig. 5) and to select the individual coupling regions by means of topological and geometrical operators. Later, the coupling information created with **FSCON** can be saved and subsequently be read by the geometric coupling tool **FSI**. The geometric coupling tool **FSI** must then ensure that the conservation of total forces, moments, and work is still maintained.

4.1 The CFD Model

Control surfaces are, for various reasons, frequently modelled in less detail in the fluid model than in the structural model. In the structural FEM model, control surfaces are usually connected to the wing box structure by means of torsional springs and rigid-body elements, but otherwise the surface itself is distinct from the wing's surface such that there is a gap between the wing box and the control surface. By contrast, in the corresponding

CFD model, the control surface may be a mere extension of the wing and there would be no gap.

The F/A-18 wing (Fig. 4) model contains two such control surfaces, the trailing edge flap (TEF) and the aileron (AIL). In the fluid model, the following simplifications have been made: The TEF shroud and the AIL shroud have been moved such that they are flush with the upper surface of the wing box. The TEF and AIL are modelled such that their upper surfaces extend directly from the respective "shrouds", while their lower surfaces are flush with the lower surface of the wing box. Thus, there is no gap at all in the fluid model as the wing consists of a set of fully connected surfaces.

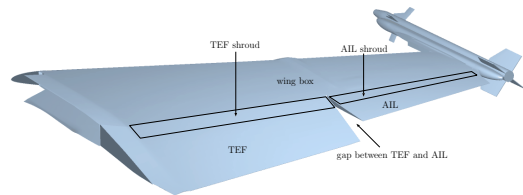


Figure 4: Simplifications in the CFD model of the F/A-18 wing.

Because of this, the different fluid coupling regions (control surfaces, wing box, etc.) have non-empty intersections, and for these intersections the deflections obtained at the fluid surface mesh points of these intersections must be identical for each adjacent coupling region.

4.2 Structural Model and Coupling Regions

Fig. 5 shows the coupling regions for the F/A-18 wing. The structural model is represented by a set of load stations, which are displayed in Fig. 5 as dots. The actual FEM mesh is considerably finer. The geometric coupling takes part through these load stations: Aerodynamic

loads are transferred to them and from their displacements, the deformation of the fluid surface is interpolated.

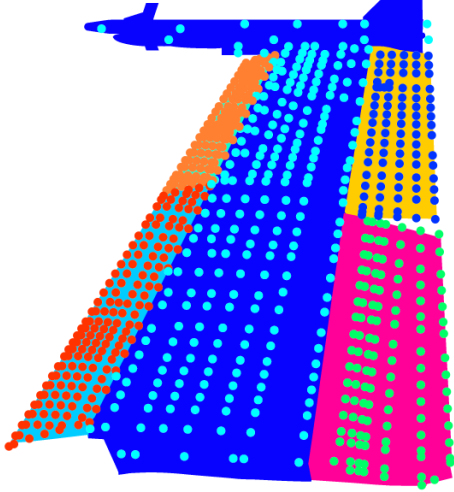


Figure 5: Fluid surface (solid) and structural coupling regions (dots) on the F/A-18 wing.

4.3 Two-region coupling

The multi-region transfer of the structural displacements to the fluid surface mesh and the transfer of the fluid surface loads to the structure is illustrated in the following. Let there be two coupling regions A and B where some of the fluid surface mesh nodes belong to both regions (Fig. 6).

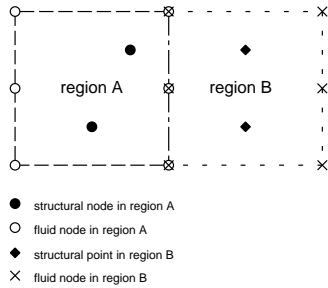


Figure 6: Two coupling regions with structural points and fluid surface mesh nodes.

The structural displacements and forces are then defined as

$$\mathbf{u}^s = \begin{Bmatrix} \mathbf{u}_a^s \\ \mathbf{u}_b^s \end{Bmatrix} \quad \text{and} \quad \begin{Bmatrix} \mathbf{f}_a^s \\ \mathbf{f}_b^s \end{Bmatrix}$$

while the fluid displacements and forces are defined

$$\mathbf{u}^f = \begin{Bmatrix} \mathbf{u}_a^f \\ \mathbf{u}_b^f \\ \mathbf{u}_i^f \end{Bmatrix} \quad \text{and} \quad \mathbf{f}^f = \begin{Bmatrix} \mathbf{f}_a^f \\ \mathbf{f}_b^f \\ \mathbf{f}_i^f \end{Bmatrix}$$

4.4 Displacement Transfer

To maintain inter-region continuity of the displacements, it is necessary to proceed in three steps. Note that steps II and step III are interchangeable.

Step I: Determine the displacements at the intersection nodes. To this end, the union of the structural nodes from regions A and B form the set of support nodes (Fig. 7).

$$\mathbf{u}_i^f = G^I \mathbf{u}^s = [G_a^I \quad G_b^I] \begin{Bmatrix} \mathbf{u}_a^s \\ \mathbf{u}_b^s \end{Bmatrix}$$

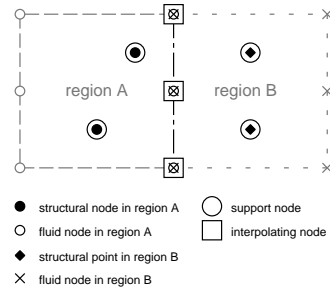


Figure 7: Transfer of displacements for step I.

Step II: The intersection nodes are then added to the structural points of region A to form an extended set of support nodes. With this new set, the displacements for the remaining fluid surface mesh nodes of region A (the

ones that are unique to region A) are obtained (Fig. 8).

$$\mathbf{u}_a^f = \underbrace{\begin{bmatrix} G_a^{II} & G_i^{II} \end{bmatrix}}_{G^{II}} \begin{Bmatrix} \mathbf{u}_a^s \\ \mathbf{u}_i^s \end{Bmatrix}$$

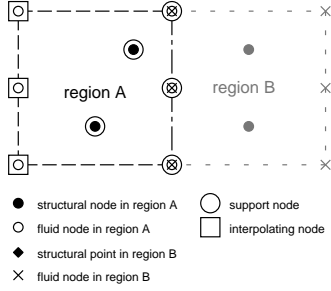


Figure 8: Transfer of displacements for step II.

Step III: The previous step is repeated for region B: The intersection nodes are added to the structural points of region B, and with this set, the displacements for the remaining fluid surface mesh nodes of region B are obtained (Fig. 9).

$$\mathbf{u}_b^f = \underbrace{\begin{bmatrix} G_b^{III} & G_i^{III} \end{bmatrix}}_{G^{III}} \begin{Bmatrix} \mathbf{u}_b^s \\ \mathbf{u}_i^s \end{Bmatrix}$$

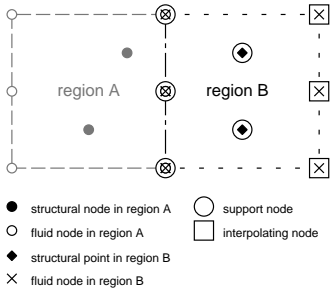


Figure 9: Transfer of displacements for step III.

If the three steps are combined into a single one, the geometric coupling procedure can be written such that a single, global coupling

operator G for the two-region problem is obtained:

$$\begin{Bmatrix} \mathbf{u}_a^f \\ \mathbf{u}_b^f \\ \mathbf{u}_i^f \end{Bmatrix} = \underbrace{\begin{bmatrix} G_a^{II} & \mathbf{0} & G_i^{II} \\ \mathbf{0} & G_b^{III} & G_i^{III} \\ \mathbf{0} & \mathbf{0} & \mathbf{I} \end{bmatrix}}_G \begin{bmatrix} \mathbf{I} & \mathbf{0} \\ \mathbf{0} & \mathbf{I} \\ G_a^I & G_b^I \end{bmatrix} \begin{Bmatrix} \mathbf{u}_a^s \\ \mathbf{u}_b^s \end{Bmatrix} \quad (3)$$

This concept can be extended to arbitrary numbers of coupling regions and region intersections.

In practice, it is more convenient to proceed in the step-wise fashion outlined above than to compute the global coupling operator G , for the reason that the explicit computation of the geometric coupling operator(s) is computationally inefficient. In either case, the coupling procedure must create the intersections and unions from the set of fluid surface nodes. The FSI tool creates the different coupling sets without requiring manual interaction; it merely reads the coupling region definitions created with FSCON and finds the intersection nodes by topological and geometrical properties. It then establishes a sequence of geometric coupling operations much in the same way as described above: First, the displacements for all intersections of regions are obtained. Then, for each coupling region, the intersection points (if any) are added to the set of support nodes, and the displacements at the remaining points are computed.

4.5 Load Transfer

For the transfer of the loads, the transpose of the coupling operators, as defined for the transfer of the displacements, must be used, for otherwise the geometric coupling will not preserve work. As with the transfer of the displacements, it is more convenient to proceed in step-wise fashion. The sequence of operations is the same, however the transfer of the forces is an additive operation.

step I: Obtain the additional forces at the fluid intersection nodes:

$$\bar{\mathbf{f}}_i^f = \underbrace{[(G_a^I)^T \quad (G_b^I)^T]}_{(G^I)^T} \begin{Bmatrix} \mathbf{f}_a^f \\ \mathbf{f}_b^f \end{Bmatrix}$$

step II: Transfer the forces from the fluid nodes of region A and the interface nodes to the structural nodes of region A:

$$\mathbf{f}_a^s = \underbrace{[(G_a^{II})^T \quad (G_i^{II})^T]}_{(G^{II})^T} \begin{Bmatrix} \mathbf{f}_a^f \\ \mathbf{f}_i^f + \bar{\mathbf{f}}_i^f \end{Bmatrix}$$

step III: Transfer the forces from the fluid nodes of region B and the interface nodes to the structural nodes of region B:

$$\mathbf{f}_b^s = \underbrace{[(G_b^{III})^T \quad (G_i^{III})^T]}_{(G^{III})^T} \begin{Bmatrix} \mathbf{f}_b^f \\ \mathbf{f}_i^f + \bar{\mathbf{f}}_i^f \end{Bmatrix}$$

The additional forces at the fluid intersection nodes $\bar{\mathbf{f}}_i^f$ are due to the fact that there is a constraint in the displacements at these nodes.

The transpose of the global coupling operator (3) is obtained by combining steps I, II, and III:

$$\begin{Bmatrix} \mathbf{f}_a^s \\ \mathbf{f}_b^s \end{Bmatrix} = G^T \begin{Bmatrix} \mathbf{f}_a^f \\ \mathbf{f}_b^f \\ \mathbf{f}_i^f \end{Bmatrix}$$

with

$$G^T = \begin{bmatrix} \mathbf{I} & \mathbf{0} & (G_a^I)^T \\ \mathbf{0} & \mathbf{I} & (G_b^I)^T \end{bmatrix} \begin{bmatrix} (G_a^{II})^T & \mathbf{0} & \mathbf{0} \\ \mathbf{0} & (G_b^{III})^T & \mathbf{0} \\ (G_i^{II})^T & (G_i^{III})^T & \mathbf{I} \end{bmatrix}$$

Hence, for any forces and displacements, work is preserved by two-region coupling. It can be shown by induction that this is the case for multi-region coupling as well.

4.6 Total force and moment

In contrast to essential boundary conditions with a zero value, two-region coupling (and thus multi-region coupling too) preserves total force and moment: If all geometric coupling operators G^I , G^{II} , and G^{III} can interpolate a constant field exactly, hence they preserve total force individually, then the combined coupling operator G preserves total force too. This can be verified by substituting a constant field for the structural displacements in (3).

If the operators G^I , G^{II} , and G^{III} are isoparametric as well, then G is isoparametric too, and hence G preserves total moment in addition to total force. This can be verified by substituting the structural coordinates for the structural displacements in (3).

Hence, multi-region coupling – if executed as described above – preserves, in addition to work, total moment and total force, if these are preserved by the interpolation scheme.

4.7 Smoothness of the fluid surface

In this section we describe how multi-region coupling can affect the smoothness of the deformed fluid surface. We define a function as smooth if it can be derived everywhere at least once (C^1). C^1 -continuity of the interpolated fluid surface deformation is important to CFD solvers, particularly if Navier-Stokes simulations are performed or if a very fine mesh is being used.

As an example for a geometric coupling operator that is not C^1 defined everywhere, we take the biharmonic volume-spline interpolant as described in [6]. This interpolant is once continuously derivable (C^1) everywhere except at the support points, where the derivative is in general not defined and thus C^0 (Fig. 10).

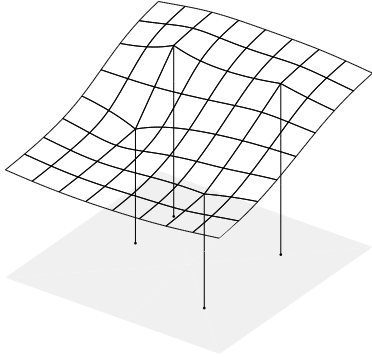


Figure 10: Interpolation of the displacement of a surface with a biharmonic volume-spline method from the displacement values defined at 4 discrete points.

Since the fluid surface mesh nodes in general do not coincide with the structural mesh nodes, of which a subset is chosen for the support points, the fact that the interpolant is only C^0 at the support points is acceptable.

In the case of multi-region coupling where there is a continuity (C^0) requirement of the displacements at the intersection of two adjacent fluid surface regions, the fluid surface points of the intersection are added to the set of support points for the interpolation of the deformation for each region, hence the interpolant becomes C^0 at the fluid surface points of the intersection. Therefore, for these kind of interpolants, coupling regions should be, if possible, defined such that the expected deformations at their intersections will be smooth.

5 Results

In this section, some of the results obtained with the geometric coupling tools `FSCON` and `FSI` in conjunction with the CFD solver `NSMB` are presented for the simulation of the aeroelastic equilibrium of the F/A-18 wing. These simulations were carried out because of lack

of sufficiently accurate aerodynamic loads data available to RUAG Aerospace [4]. Of particular interest was the effect of the deformed wing on the aerodynamic loads.

5.1 Tool chain

The computational tool chain consisted of the `NSMB` CFD solver and mesh deformation tool, the `FSCON` and `FSI` geometric coupling tools, and the structural solver `MSC.Nastran`. The simulations have been carried out on existing CFD and FEM models. Later the CFD model was re-generated from scratch with a considerably finer mesh of ≈ 14 million cells. Both CFD and FEM models allow to vary the aircraft configuration (inclination of control surfaces, loads) up to a certain amount; for a set of configurations the corresponding CFD and FEM models were generated and the aeroelastic simulation was set up and carried out.

Each simulation consisted of several iterations, until sufficient convergence of the deformations was achieved. Typically 3 or 4 iterations were required. Each iteration in turn consisted of the following steps:

1. Compute the steady flow field for the current volume mesh with `NSMB`.
2. Transfer the aerodynamic loads to the structure with `FSI`.
3. Compute static equilibrium of the structure under these loads with `MSC.Nastran`.
4. Transfer the structural displacements to the fluid surface mesh with `FSI`.
5. Deform the fluid volume mesh according to the fluid surface displacements with `FSI`.

Before running a simulation, the multi-region coupling was defined with `FSCON`, see Fig. 5. The fuselage and the horizontal and

vertical tail were not coupled, and therefore were considered rigid. At the wing root, the fluid surface displacements were constrained to zero to yield a smooth deformed fluid surface, such that the fluid volume-mesh deformation was able to produce a valid volume-mesh for the next iteration.

For the geometric coupling, a biharmonic volume-spline method as described in [6] was used. This is a variant of radial basis function interpolation that interpolates constant fields exactly, thus preserves total force but not total moment. The error in the moments was very small however, since the structural points cover almost the whole fluid surface.

5.2 C1S825 load case

The results presented in this paper were obtained for the C1S825 load case, which corresponds to a 8.25g steady-state manoeuvre, with the leading edge flap rotated by 17.4 degrees and the trailing edge flap rotated by 13.4 degrees. The angle of attack is 15.9 degrees. The case is considered symmetric, only half of the aircraft is modelled. Far field pressure is 84300[Pa], corresponding to an altitude of 5000[m]. The mach number is 0.7.

The total force and moment are, due to the effect of the deformation on the air flow, reduced by 15% for the force and by 16% for the bending moment at the wing root.

Fig. 11 displays the undeformed and the deformed fluid surface. The displacement is of the pure bending type. The angle between the trailing edge flap (TEF) and the aileron (AIL) is significantly reduced in the deformed state.

The surface remains continuous across the region borders (transition between TEF and wing box, transition between AIL and wing box). Where the undeformed surface is smooth, that smoothness is retained in the deformed surface.

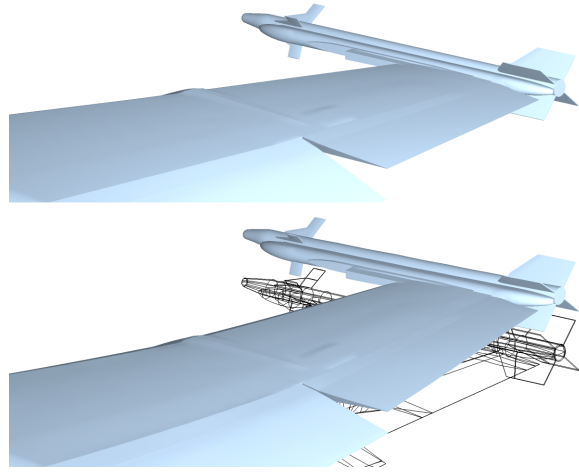


Figure 11: Undeformed (top) and deformed (bottom) fluid surface.

Fig. 12, a cut through the undeformed and the deformed fluid surface, shows the differences in the deformation of the TEF and AIL control surfaces; while the AIL deformation is hardly visible, the TEF is, on the outboard side, rotated such that the angle with the aileron is reduced.

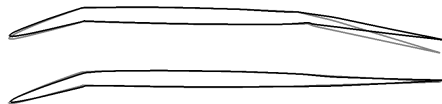


Figure 12: Undeformed (grey) and deformed (black) wing profile at 3.5[m] depth from symmetry plane (top) and at 4.0[m] depth (bottom).

Fig. 13 displays the difference in the pressure field between the deformed and the undeformed surface. On the upper surface, the pressure variation is small, except at the in-board leading edge where it is decreased, and at the outboard leading edge flap where it is increased. On the lower surface, pressure is significantly reduced in the wing box region and at the trailing edge flap (TEF). The latter can

be expected from the rotation of the TEF in the deformed model.

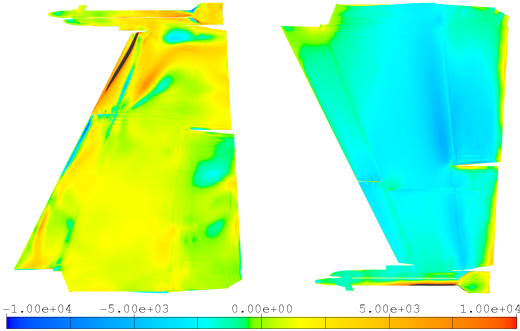


Figure 13: Pressure difference between the undeformed and the deformed wing for the upper (left) and lower (right) wing surface.

Finally, skin friction surface streamlines are displayed (Fig. 14).

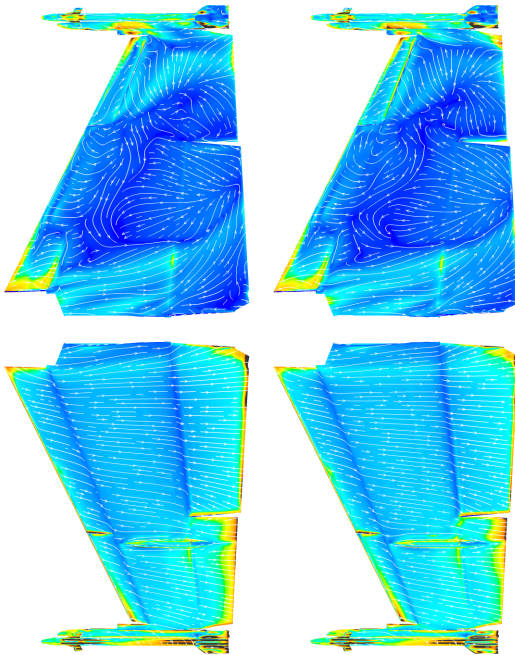


Figure 14: Skin friction streamlines for the upper (top) and lower (bottom) surface of the undeformed (left) and the deformed (right) wing.

6 Conclusion and outlook

The time-domain aero-elastic tool chain presented in this paper is well suited for aerodynamically demanding problems; the staggered scheme allows for using advanced, non-linear CFD and CSM solvers. In the context of the F/A-18 wing simulations, the ability to predict shock boundaries and to handle turbulence effects was of particular importance for obtaining accurate results. By contrast, classical aero-elastic tools based on linear theory will – for such flow regimes – fail to produce results with sufficient accuracy.

On the other hand, time-domain methods require a much higher computational effort and the time for preparing of the highly detailed CFD and CSM models has to be taken in account. The overall cost of such aero-elastic simulations is thus very high. In comparison, the time needed to set up the geometric coupling and the computational effort of the geometric coupling is small. For the aero-elastic simulations presented in this paper, 98% of the elapsed time was spent on CFD and mesh deformation, the coupling and structural analysis being negligible. The small computational effort for the geometric coupling can be explained by the relatively small number of data points used and the efficient computer implementation of the coupling program.

At the time of writing this paper, efforts were going on to extend the concepts and the tool chain presented in this paper to non-stationary aero-elastic simulations. A prototype had been established and validated at the beginning of 2006. The prototype is currently being improved to permit fully implicit aero-elastic, synchronous coupling. The aero-elastic methods outlined in this paper will be applied to flow regimes at high angles of attack, the aim of such simulations being the evaluation of the aerodynamic forces acting on the vertical tail of the F/A-18 aircraft, specifically the con-

tribution of the vortex generated by the leading edge extension (LEX). Different manoeuvres at various angles of attack will be simulated, thus establishing fatigue spectra for assessing the vertical tail root, a critical part.

Finally, the tool chain will be used to simulate the complete aircraft under non-stationary conditions where the unsteady flow interacts with the deformable structure, the goal being to study instabilities due to buffet loads.

analysis, TP 95690U, p. 18-19. Tech. rep., National Aerospace Laboratory NLR, Amsterdam, The Netherlands, 1995.

- [7] SIBSON, R. A vector identity for the dirichlet tessellation. In *Mathematical Proceedings of the Cambridge Philosophical Society* (87:151-155, 1980).

References

- [1] ARMIN BECKERT AND HOLGER WENDLAND. Multivariate Interpolation for Fluid-Structure-Interaction Problems Using Radial Basis Functions, 2001.
- [2] GERMAINE STANISLASSE LAURE GOURA. *Time-Marching Analysis of Flutter using Computational Fluid Dynamics*. PhD thesis, Department of Aerospace Engineering, University of Glasgow, 2001.
- [3] J.B. VOS, A.W. RIZZI, A. CORJON, A. CHAPUT, E. SOINNE. Recent advances in aerodynamics inside the NSMB (Navier Stokes multiblock) consortium. Tech. rep., American Institute of Aeronautics, Inc., AIAA-98-0225.
- [4] M. GUILLAUME, A. GEHRI, B. BUCHER, J.B. VOS, S. MERAZZI, TH. LUDWIG, G. MANDANIS. Calculation of F/A-18 fatigue loads and wing deformation using computational fluid dynamics, 2006.
- [5] MARTIN D. BUHMANN. *Radial Basis Functions*. Cambridge University Press, New York, NY, USA, 2003.
- [6] M.H.L. HOUNJET, J.J. MEIJER. Evaluation of elastomechanical and aerodynamic data transfer methods for non-planar configurations in computational aeroelastic